2022-1243 IJOI
https://www.ijoi-online.org/

International Journal of Organizational Innovation

SHEAR BAND CONDITIONS REQUIRED TO DEVELOP THE EQUATION FOR THE ULTIMATE BEARING CAPACITY OF A STRIP FOUNDATION

Tse-Shan Hsu
President, Institute of Mitigation for Earthquake Shear Banding Disasters
Professor, Feng-Chia University, Taiwan
tshsu@fcu.edu.tw

Zong-Lin Wu, Yu-Chien Wu
Directors, Institute of Mitigation for Earthquake Shear Banding Disasters, Taiwan

Da-Jie Lin, Tsai-Fu Chuang
Associate Professors, Feng-Chia University, Taiwan

Yi-Min Huang
Assistant Professor, Feng-Chia University, Taiwan

Abstract

Evaluation of the ultimate bearing capacity of a strip foundation requires the incorporation of the shear bands. However, when the applied force reaches the ultimate load, the shear bands that should be induced from localizations of deformations do not appear when expected. In view of this, in this paper, the following four conclusions are drawn based on the characteristics of the solutions of the static equilibrium equation under stable and unstable conditions. (1) Using the plastic strain hardening model or the perfectly plastic model, the elastic-plastic solution is obtained under stable conditions, so shear bands cannot be induced and the structural symmetry is maintained. (2) Using the plastic strain softening model, the elastic-plastic solution

is obtained under unstable conditions and with the prescribed displacements, so shear bands are induced and the structural symmetry is lost. (3) In the development of the traditional equation for the ultimate bearing capacity of a strip foundation, the perfectly plastic model, which cannot induce shear bands, is adopted when the incorporation of shear bands is required, so the ultimate bearing capacity that meets the needs of the actual situation cannot be obtained by applying the developed equation. (4) In the case of using the perfectly plastic model, when the foundation load reaches the ultimate load, the plastic strain zone expands in an unduly symmetric manner, and the estimated ultimate bearing capacity of the strip foundation is therefore unduly high. Based on the above four conclusions, it is suggested that future evaluation of the ultimate bearing capacity of strip foundations must adopt the plastic strain softening model. Only in this way will the evaluated ultimate bearing capacity of the strip foundation meet the safety requirements.

Keywords: strain softening, perfectly plastic, ultimate bearing capacity, foundation, stable conditions, unstable conditions, symmetry.

Introduction

Earthquakes can be divided into five types: tectonic earthquakes, volcanic earthquakes, subsidence earthquakes, reservoir-induced earthquakes, and artificial explosion-induced earthquakes (China Earthquake Disaster Prevention Center, 2017). The main effect of tectonic earthquakes is shear banding, and its energy proportion is greater than 90% of the total energy of the tectonic earthquake. The secondary effect is ground vibration, and its energy proportion is less than 10% of the total energy of the tectonic earthquake (Coffey, 2019).

The building code for foundation seismic design stipulates that the safety factor of the bearing capacity of a strip foundation must be greater than or equal to 1.2 during earthquakes, and greater than or equal to 3.0 under normal conditions (Construction and Planning Agency, Ministry of the Interior of Taiwan, 2001, 2011). For building foundations situated in alluvial sandy silt layers, provided that the foundations adhere to the code requirements, they will not tilt or collapse because of an insufficient ultimate bearing capacity, regardless of the conditions, as they would have been designed to be re-

sistant to ground vibration.

However, even if a building is symmetric under normal conditions (detailed in Figure 1), the foundation soil still loses its ellipticity during the strain softening process that occurs during tectonic earthquakes, the static equilibrium equation departs from a stable condition, and the structural matrix loses its symmetry. Therefore, the shear resistance strength of the foundation soil is reduced from the peak value to the residual one, resulting in asymmetric general shear failure occurring in the building foundation (detailed in Figure 2), which will induce building tilt failure (detailed in Figure 3).

Figure 1. A symmetric and stable building under normal conditions.

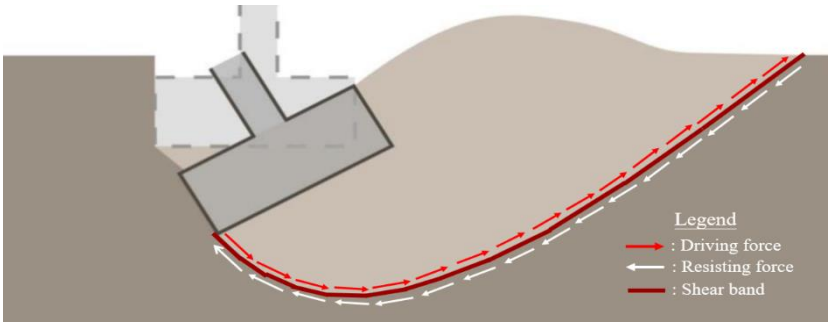

Figure 2. General shear failure of the strip foundation under asymmetric and unstable conditions.

Figure 3. Tilt failure of buildings induced by tectonic earthquakes (Hsu and Ho, 2016).

For an overall structure including the building, foundation, and foundation soils, the static equilibrium equation is $\boldsymbol{K}_{ij}d\boldsymbol{x}_j = d\boldsymbol{F}_j$, where $\boldsymbol{K}_{ij}$ is the structure matrix, $d\boldsymbol{x}_j$ is the incremental displacement vector, and $d\boldsymbol{F}_j$ is the incremental force vector.

For an overall structure under normal conditions, when $i \neq j$, the entries $k_{ij} = k_{ji}$ when the overall structure matrix $\boldsymbol{K}_{ij}$ is symmetric. Assuming that $d\boldsymbol{x}_j^1$ and dx_j^2 are both solutions of $\boldsymbol{K}_{ij}d\boldsymbol{x}_j = d\boldsymbol{F}_j$, then $\boldsymbol{K}_{ij}d\boldsymbol{x}_j^1 = d\boldsymbol{F}_j$ and $\boldsymbol{K}_{ij}d\boldsymbol{x}_j^2 = d\boldsymbol{F}_j$ are true simultaneously, and therefore $\boldsymbol{K}_{ij}(d\boldsymbol{x}_j^1 - d\boldsymbol{x}_j^2) = \boldsymbol{0}$ can be obtained.

First, under the stable condition when the determinant of the structure matrix $|\boldsymbol{K}_{ij}| \neq 0$, then $d\boldsymbol{x}_j^1 - d\boldsymbol{x}_j^2 = \boldsymbol{0}$, and therefore the unique solution $d\boldsymbol{x}_j^1 = d\boldsymbol{x}_j^2 = d\boldsymbol{x}_j$ can be obtained. Secondly, under the unstable conditions when the determinant of the structure matrix $|\boldsymbol{K}_{ij}| = 0$, the solution containing shear bands can be obtained under the conditions of the prescribed displacements (Hsu, et al., 2022).

For an overall structure that is symmetric under normal conditions, when plastic strain softening induces conditions such that $|\boldsymbol{K}_{ij}| = 0$ during

tectonic earthquakes, the entries of two adjacent rows of the overall structure matrix $\boldsymbol{K}_{ij}$ have the relationship of $k_{ij} = k_{i+1\,j}$, and so the solution containing shear bands is asymmetric (Hsu, et al., 2022).

When past scholars (Prandtl, 1920; Terzaghi, 1943; Meyerhof, 1951, 1963; Hansen 1970; Vesic, 1973) developed the equation of the ultimate bearing capacity of a strip foundation, they should have used an asymmetric shear band (shown in Figure 2), but instead improperly used a shear band associated with the symmetric general shear failure shown in Figure 4.

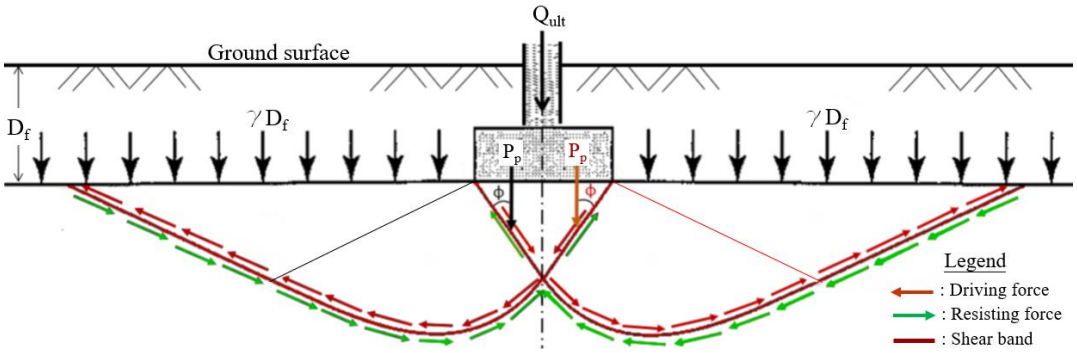

Figure 4. The assumed symmetric shear band associated with the general shear failure of the strip foundation (reproduced from Terzaghi, 1943).

For strip foundations, McCarthy (2007) showed that the shear band associated with general shear failure occurs only in dense sand or firm clay. In Figure 4, Q_{ult} is the ultimate load, P_p is the passive earth pressure, $\emptyset$ is the internal friction angle, γ is the unit weight of the soil, and D_f is the embedded depth of the foundation.

Figure 5 shows the load–settlement curve related to the general shear failure of the strip foundation. It can be seen from Figure 5 that when the settlement is greater than that corresponding to the peak load, the load that the dense sand or the firm clay can withstand decreases as the settlement increases.

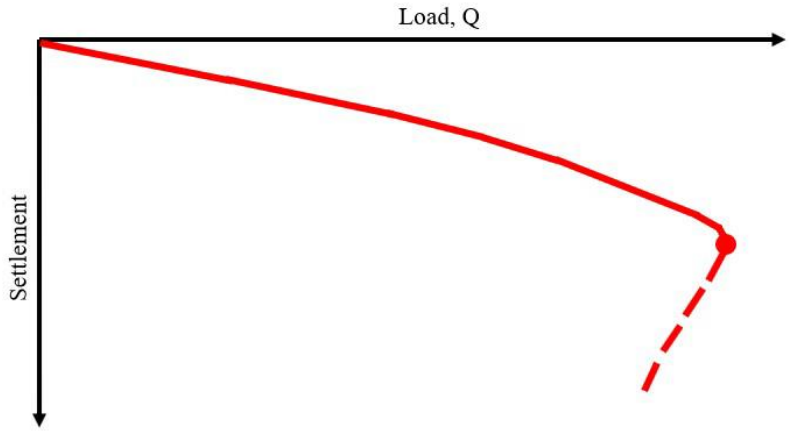

Figure 5. Load–settlement curve for general shear failure of a strip foundation (reproduced from McCarthy, 2007).

Figure 6 shows the perfectly plastic model used in the development of the ultimate bearing capacity of the strip foundation. It can be seen from Figure 6 that, when the stress reaches the ultimate value, it remains constant as the strain increases.

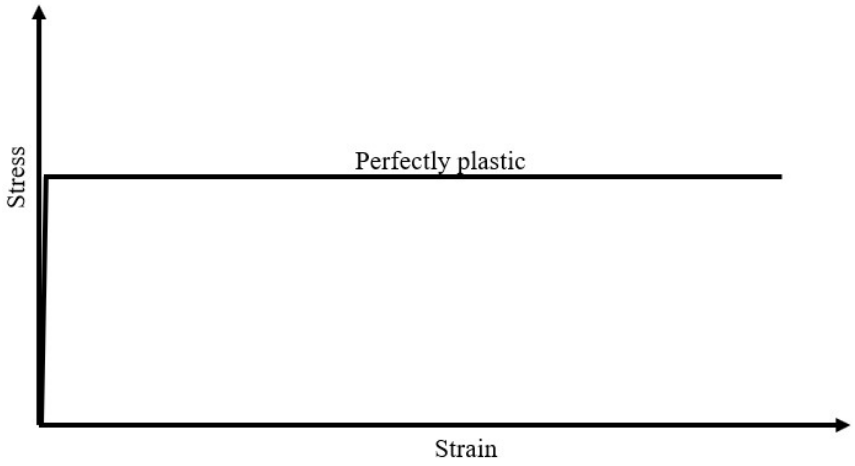

Figure 6. The stress–strain relationship for the perfectly plastic model (reproduced from Terzaghi, 1943).

McCarthy (2007) asserted that the perfectly plastic model shown in Figure 6 only occurs during punching shear failure of loose sand or soft clay (detailed in Figure 7). Therefore, by comparing Figures 5 and 6 it can be deduced that in the development of the ultimate bearing capacity of the strip foundation, the scholars referred to above (Prandtl, 1920; Terzaghi, 1943; Meyerhof, 1951, 1963; Hansen 1970; Vesic, 1973) improperly used the perfectly plastic model when the plastic strain softening model should have been used instead.

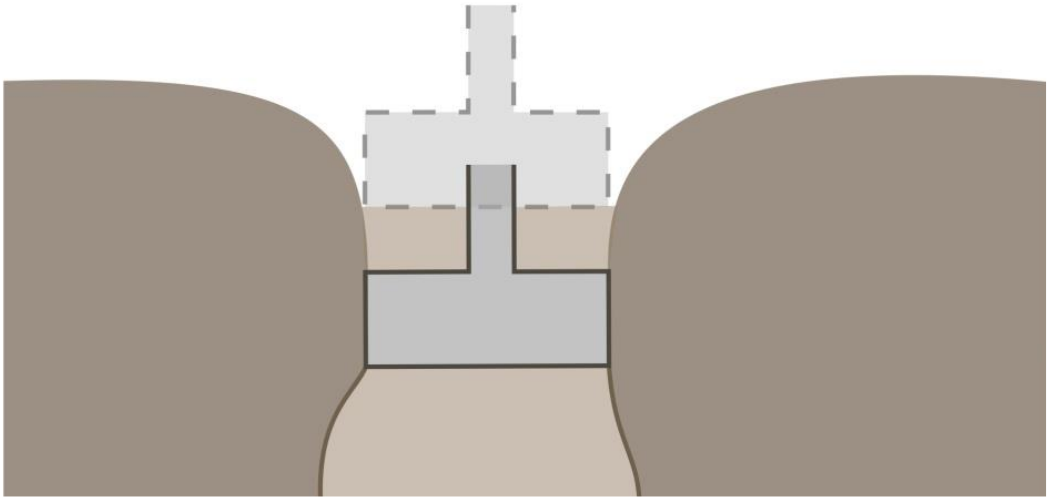

Figure 7. Punching shear failure of loose sand or soft clay.

In view of the above-mentioned problems arising from the use of the perfectly plastic model and the symmetric shear band in the development of the traditional equation of ultimate bearing capacity of strip foundations, it is important to further explore the characteristics of the solution of the static equilibrium equation under plastic stable and plastic unstable conditions.

Numerical Solution of Static Equilibrium Equation

The Adopted Constitutive Equation

First the yield function proposed by Hsu (1987) is used:

$$F = J_{2D}^{1/2} - \left(\kappa + H\,\gamma_{oct}^{P}\right) = 0 \qquad \text{(Equation 1)}$$

where

J_{2D} = the second invariant of deviatoric stress;

J_{2D} = the second invariant of deviatoric stress;

κ = the size of the initial yield surface;

γ_{oct}^{p} = the plastic octahedral shear strain;

$H/2G$ = the strain softening parameter;

G = the shear modulus.

Secondly, the stress–strain matrix proposed by Hsu (1987) is adopted:

$$\begin{aligned}\overline{D}_{ijkl}^{ep} &= \overline{D}_{ijkl}^{e} - \overline{D}_{ijkl}^{p} \\ &= \overline{D}_{ijkl}^{e} - \overline{D}_{ijkl}^{e}\frac{\partial F}{\partial \sigma'_{kl}}\frac{\partial F}{\partial \sigma'_{ij}}\overline{D}_{ijkl}^{e}\left[\frac{1}{\sqrt{6}}H + \frac{\partial F}{\partial \sigma'_{ij}}\overline{D}_{ijkl}^{e}\frac{\partial F}{\partial \sigma'_{kl}}\right]^{-1}\end{aligned} \qquad \text{(Equation 2)}$$

Problem Description

A uniform symmetric 50×25 mesh under the conditions of uniformly prescribed displacements is used to analyze the behavior of a 5.08 cm × 2.54 cm plate (shown in Figure 8) under plane strain conditions loaded at both ends, where the movement in the direction perpendicular to the loading is constrained.

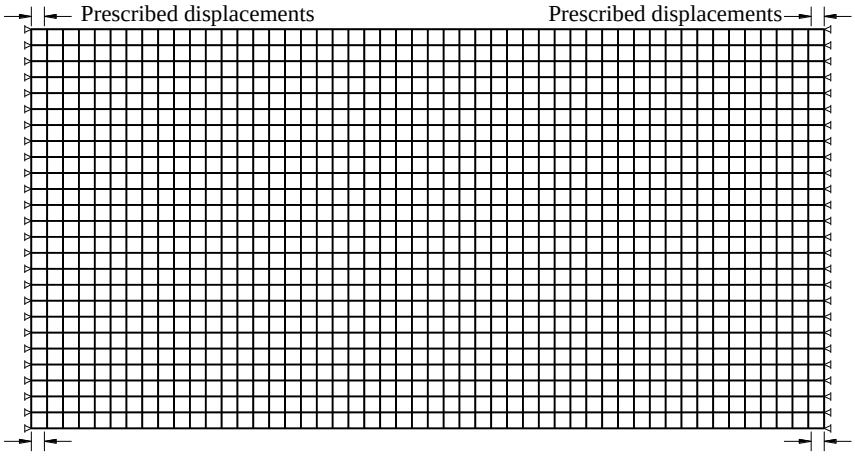

Figure 8. The finite-element mesh, boundary conditions, and prescribed lateral displacements (Hsu *et al*., 2016).

The material properties adopted are as follows:

1) The initial size of yield surface, κ, is equal to 24kPa;
2) The Young's modulus, *E*, is equal to 1200kPa;
3) Poisson's ratio, ν, is equal to 0.3;
4) The shear modulus, *G*, is equal to 462kPa;
5) The bulk modulus of water, B_w, is equal to 2140MPa;
6) The strain hardening parameter, *H*/2*G*, is equal to 0.05, 0.0, and −0.05 for strain hardening, perfectly plastic, and strain softening conditions, respectively.

Numerical Results under Plastic Stability Conditions

1) *H*/2*G* = 0.05

When using H/2G = 0.05, since the inner product $d\boldsymbol{\sigma} : d\boldsymbol{\varepsilon}_p \geq 0$ of the stress increment $d\boldsymbol{\sigma}$ and the plastic strain increment $d\boldsymbol{\varepsilon}_p$, it is known from Drucker's stability postulate that the analysis of the static equilibrium equation should be carried out under plastic stable conditions. The resulting deformed finite-element mesh, the distribution of the velocity vectors, and the distribution of the strain energy density contours obtained analytically are shown in Figures 9 to 11.

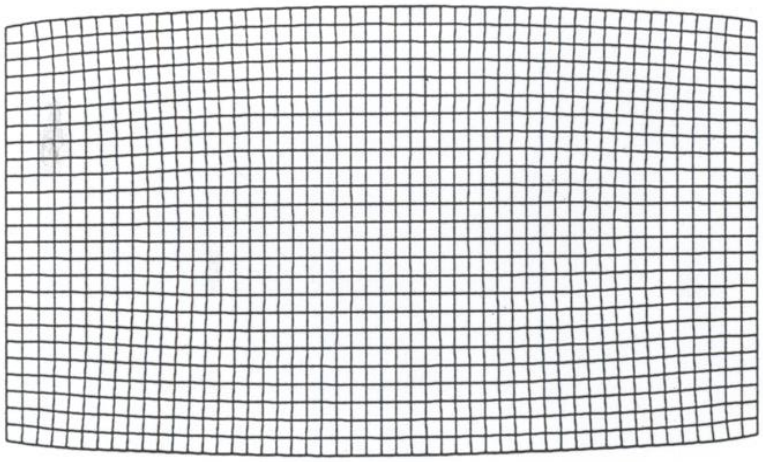

Figure 9. Deformed finite-element mesh for *H*/2*G* = 0.05 (Hsu *et al.*, 2021).

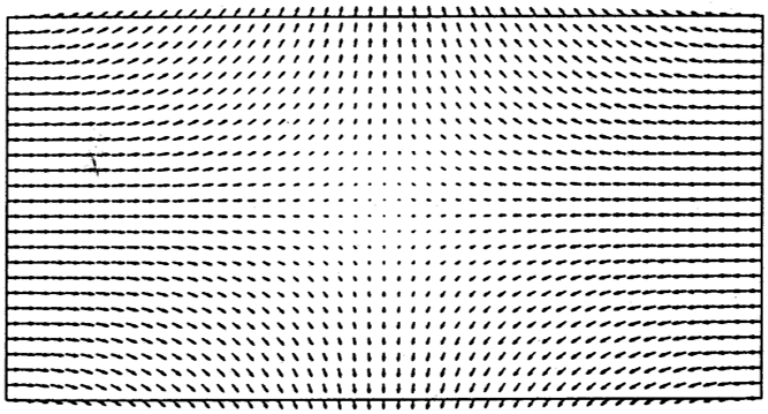

Figure 10. Distribution of the velocity vectors for $H/2G = 0.05$.

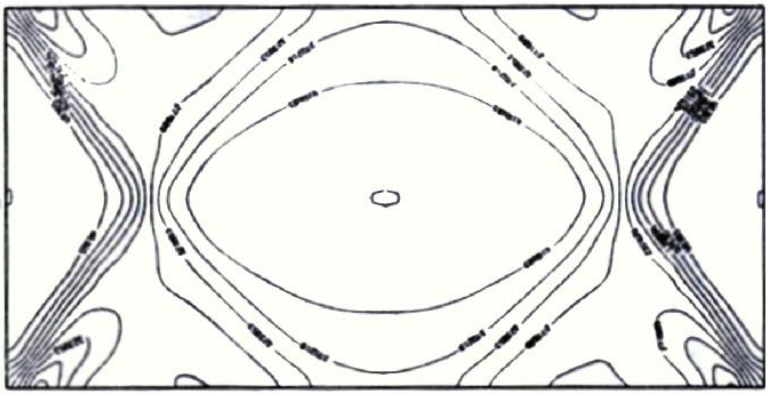

Figure 11. Distribution of the strain energy density contours for $H/2G = 0.05$.

2) $H/2G = 0.0$

When using $H/2G = 0.0$, since the inner product $d\boldsymbol{\sigma} : d\boldsymbol{\varepsilon}_p \geq 0$ for the stress increment $d\boldsymbol{\sigma}$ and the plastic strain increment $d\boldsymbol{\varepsilon}_p$, it is known from Drucker's stability postulate that the analysis of the static equilibrium equation should be carried out under plastic stable conditions. The resulting deformed finite-element mesh, the distribution of the velocity vectors, and the distribution of the strain energy density contours obtained analytically are shown in Figures 12 to 14.

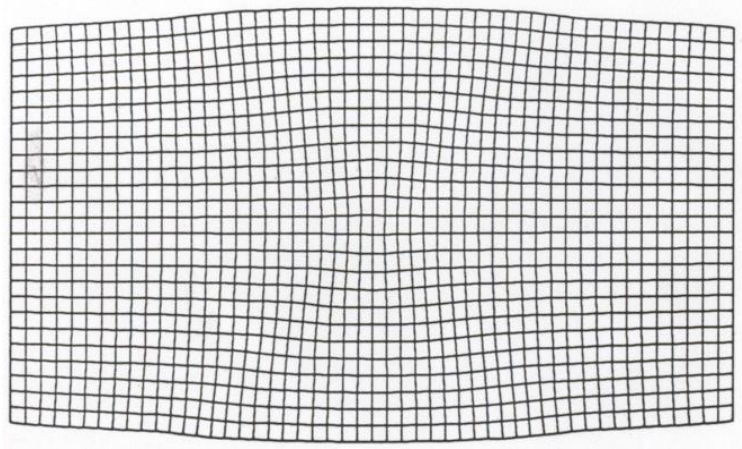

Figure 12. Deformed finite-element mesh for $H/2G$ = 0.0 (Hsu *et al.*, 2021).

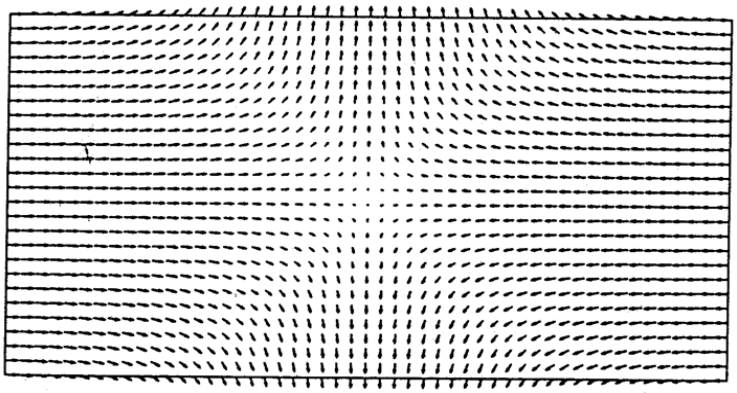

Figure 13. Distribution of the velocity vectors for $H/2G$ = 0.0.

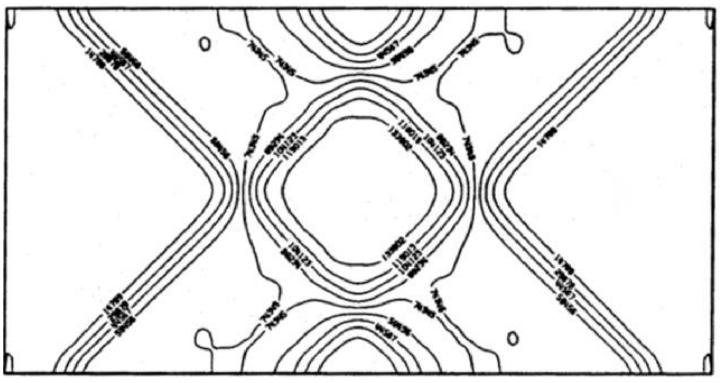

Figure 14. Distribution of the strain energy density contours for $H/2G$ = 0.0.

Numerical Results under Plastic Instability Conditions

When using $H/2G = -0.05$, since the inner product $d\boldsymbol{\sigma} : d\boldsymbol{\varepsilon}_p < 0$ of the stress increment $d\boldsymbol{\sigma}$ and the plastic strain increment $d\boldsymbol{\varepsilon}_p$, it is known from Drucker's stability postulate that analysis of the static equilibrium equation should be carried out under plastic unstable conditions. The resulting deformed finite-element mesh, the distribution of the velocity vectors, and the distribution of the strain energy density contours obtained analytically are shown in Figures 15 to 17.

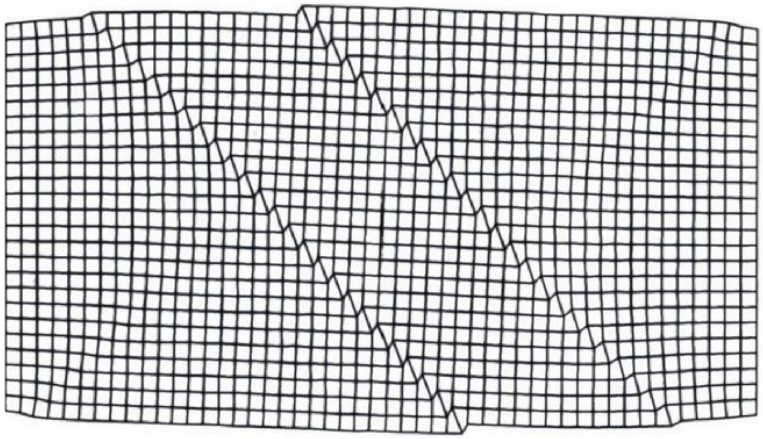

Figure 15. Deformed finite-element mesh for $H/2G = -0.05$ (Hsu *et al*., 2017).

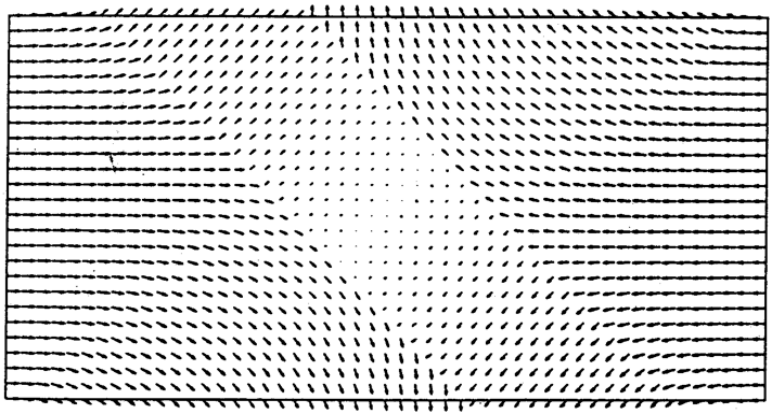

Figure 16. Distribution of the velocity vectors for $H/2G = -0.05$.

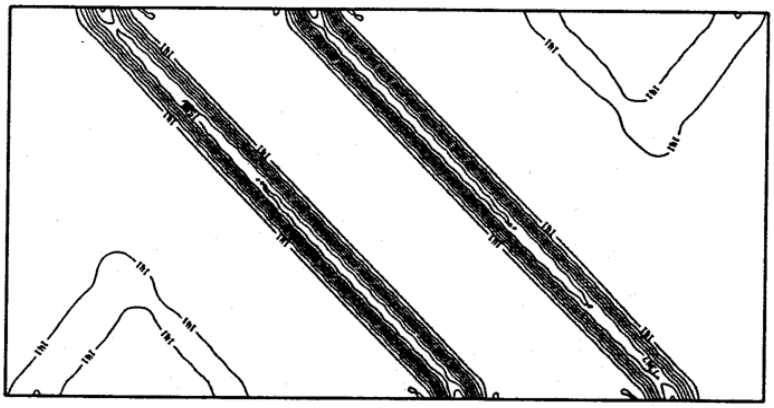

Figure 17. Distribution of the strain energy density contours for $H/2G = -0.05$ (Hsu *et al*., 2017).

Comparison and Discussion of Results

1) Although the symmetric deformed meshes (detailed in Figures 9 and 12) are obtained using the strain hardening model and the perfect plastic model under the same prescribed lateral displacement conditions, none of the obtained deformed meshes contain shear bands, whereas the asymmetric deformed mesh (detailed in Figure 15) is obtained using the plastic strain softening model and the obtained deformed mesh actually contains shear bands.

2) The distributions of the velocity vectors obtained can be compared for when $H/2G$ is equal to 0.05, 0.00, and −0.05. By comparing Figures 10, 13, and 16, it can be seen that the unevenness of the velocity vector distributions increases with the decrease of $H/2G$. When $H/2G$ decreases from 0.00 to −0.05, the unevenness of the distribution of velocity vectors increases greatly and the distribution of velocity vectors also change from a symmetric distribution to an asymmetric distribution because the analysis conditions change from stable conditions to unstable conditions. In the case of an asymmetric distribution of the velocity vectors, slip-type shear bands appear that have vectors in the same direction though different in size, as do twinning-type shear bands that have vectors of the same size though different in direction.

3) The distributions of the different

strain energy density contours obtained can be compared for when $H/2G$ is equal to 0.05, 0.00, and −0.05. From Figures 11, 14, and 17, it can be seen that the distribution nonuniformity of the strain energy density contours increases as $H/2G$ decreases. When $H/2G$ decreases from 0.00 to −0.05, the distribution nonuniformity of the strain energy density contours increases greatly because the analysis conditions change from stable conditions to unstable conditions. The distribution of the strain energy density contours also changes from a symmetric distribution to an asymmetric distribution, and shear bands appear in the area where the distribution of strain energy density contours is highly dense.

4) Given that the shear bands are induced by localization of deformations, Figures 2, 4, and 17 show that the plastic strain zones only exist in the shear bands, and the areas outside the shear bands are elastic strain zones (detailed in Figure 18).

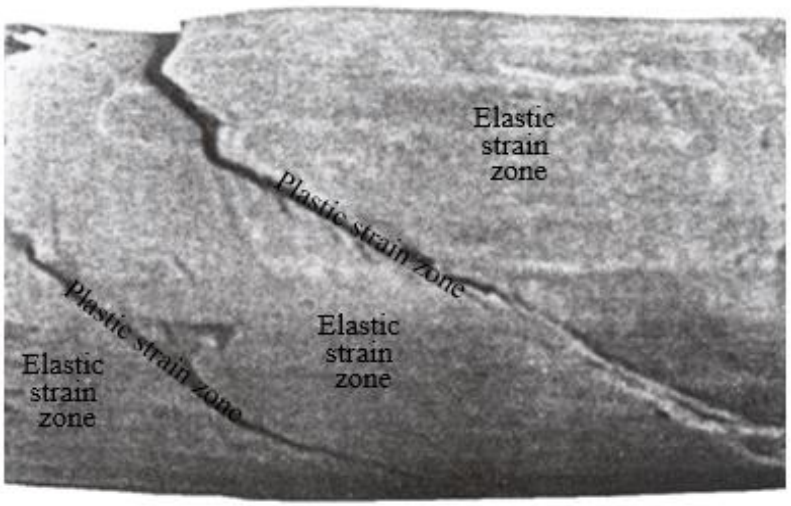

Figure 18. Elastic and plastic strain zones in a deformed mudstone sample.

5) Figure 19 shows distribution of plastic strain zones obtained from finite element analysis under elastic-perfectly plastic model (Chen, 1975). It can be seen from Figure 19 that the plastic strain zones of the foundation soil continue to expand with the increase of the load, but

there is no tendency for localizations of deformations, so shear bands cannot be induced in the plastic strain zones.

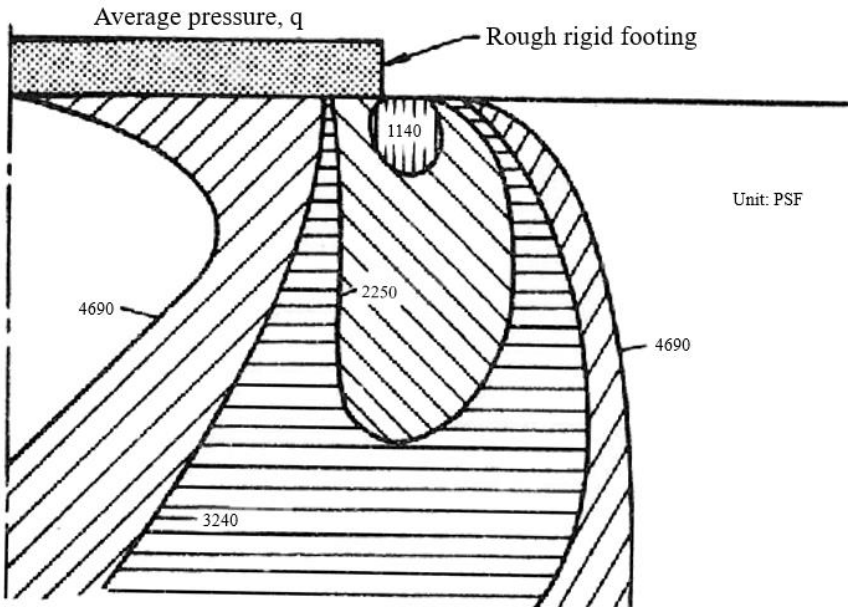

Figure 19. Distribution of plastic strain zones obtained from finite-element analysis using an elastic-perfectly plastic model (Chen, 1975).

6) Figure 20 shows the field of velocity vectors under the ultimate load of the strip foundation (Chen, 1975). The artificially drawn symmetrical shear bands pass through suitably small visible velocity vectors. Such shear bands are completely different from the slip and twinning shear zones shown in Figure 16. In addition, since the shear bands only exist under the unstable conditions of the plastic strain softening model, it is meaningless to artificially draw shear bands in the velocity vector field obtained under the stable conditions of the perfectly plastic model (detailed in Figure 20).

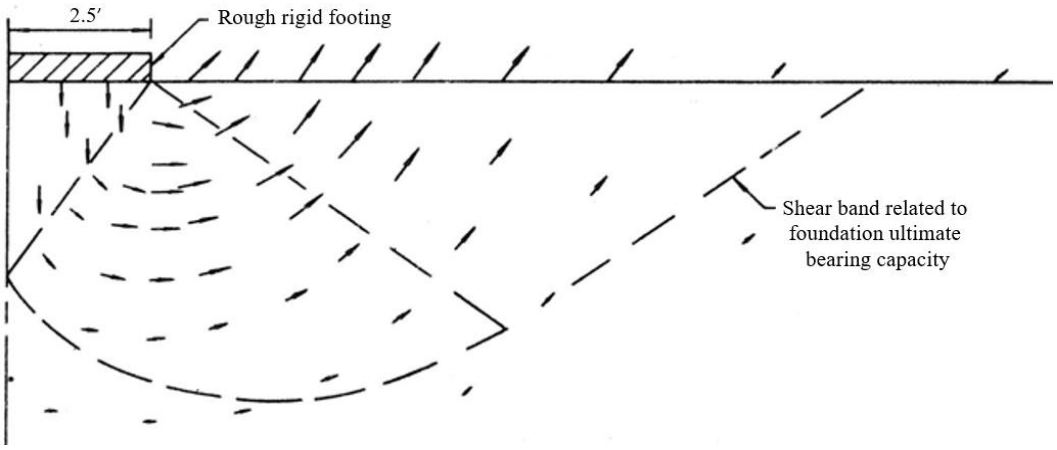

Figure 20. The velocity field induced by the ultimate load of the foundation (Chen, 1975).

7) The deformed meshes shown in Figures 9 and 12, the distributions of the velocity vectors shown in Figures 10 and 13, and the strain energy density contours shown in Figures 11 and 14 all show that shear bands do not occur under the stable conditions that occur when $H/2G = 0.00$ and $H/2G = 0.05$. The deformed mesh shown in Figure 11, the distribution of the velocity vectors shown in Figure 14, and the strain energy density contours shown in Figure 17 all show that shear bands do appear under the unstable conditions that occur when $H/2G = -0.05$. Therefore, in the development of the equation for the ultimate bearing capacity of the strip foundation, the strain softening model must be used instead of the perfectly plastic model when shear band coordination is required.
8) When the width of the strip foundation is B = 4 m, the embedding depth is $D_f = 3$ m, and the unit weight of the foundation soil is $\gamma = 20$ kN/m^3, then the peak cohesion $c_p = 15$ kPa, the residual cohesion $c_r = 0$ kPa, the peak internal friction angle $\emptyset_p = 34°$, and the residual internal friction angle $\emptyset_r = 30°$. According to Terzaghi (1943), when $\emptyset_p = 34°$, the bearing capacity factors of the strip foundation $N_c = 42.2$, $N_q = 29.4$, and $N_\gamma = 41.1$; when $\emptyset_r = 30°$, the bearing capacity factors of the strip foundation $N_q = 18.4$ and $N_\gamma = 22.4$. Then, using the traditional equation of the ultimate bearing capacity of the strip founda-

tion, the result $q_u = cN_c + qN_q + \frac{1}{2}B\gamma N_\gamma = 4041$ kPa is obtained for $c_p = 15$ kPa and $\emptyset_p = 34°$. However, first, because shear bands appear after the strain goes deep into the plastic range, the residual shear resistance strength parameters should be used, where $\emptyset_r = 30°$, $c_r = 0$ kPa. Second, because the shear band is asymmetric, the ultimate bearing capacity of the strip foundation is only half of $q_u = qN_q + \frac{1}{2}B\gamma N_\gamma$; in other words, the result $q_u = \frac{1}{2}\left(qN_q + \frac{1}{2}B\gamma N_\gamma\right) = 1000$ kPa is obtained. Therefore, this case shows that the application of the traditional equation of the ultimate bearing capacity of the strip foundation will seriously overestimate the ultimate bearing capacity of the strip foundation by 3041 kPa.

Conclusions and Suggestions

Generally, in the design of a building foundation, the ultimate bearing capacity of the strip foundation, must first be calculated and so it is important to evaluate the correctness of the equation used to do this. In view of this, in this paper, the problems arising from the use of symmetric shear bands and the perfectly plastic model in the development of the traditional equation of the ultimate bearing capacity of the strip foundation were studied. The results led to the following four conclusions:

1) In the plastic strain hardening model and the perfectly plastic model, since $d\boldsymbol{\sigma} : d\boldsymbol{\varepsilon}_p \geq 0$, the static equilibrium equation was solved under conditions such that Drucker's stability postulate is satisfied. The obtained solutions, including the deformed meshes, the distributions of velocity vectors, and the strain energy density contours, were all symmetric, but none of the shear bands appeared.

2) Using the plastic strain softening model, since $d\boldsymbol{\sigma} : d\boldsymbol{\varepsilon}_p < 0$, the static equilibrium equation was solved under unstable conditions and with the prescribed displacements. The obtained solutions, including the deformed meshes, the distribution of the velocity vectors, and the strain energy density contours, were all asymmetric, and all of them clearly showed shear bands.

3) In the case where both the shear band and the perfectly plastic model are adopted at the same time, and also in the case where the shear band cannot be induced under stable conditions, the traditionally developed equation to calculate the ulti-

mate bearing capacity of the strip foundation cannot produce a result that meets the actual safety requirements.

4) In the case of using a perfectly plastic model, when the foundation load reaches the ultimate load, the plastic strain zone expands symmetrically and in an undesired manner since the deformations cannot be localized and the originally symmetric structure cannot be transformed into an asymmetric one when foundation failure occurs. These inaccurate results lead to an excessively large overestimation of the ultimate bearing capacity of the strip foundation.

Based on the above four conclusions, it is suggested that the equation of the ultimate bearing capacity of the strip foundation developed from the plastic strain softening model and asymmetric shear band presented in this paper should be used in the future. Only in this way will the ultimate bearing capacity equation meet the actual design requirements. Thus, ensuring that the building will not tilt or collapse as a result of shear banding during tectonic earthquakes and the insufficient ultimate bearing capacity of the strip foundation.

References

Chen, W. F., *Limit Analysis and Soil Plasticity*, Elsevier Scientific Pub. Co.: Amsterdam, The Netherlands; New York, NY, USA, 1975.

China Earthquake Disaster Prevention Center, "How does earthquake happen? Type of earthquakes," China Digital Science and Technology Museum: Earthquake, Website: http://amuseum.cdstm.cn/AMuseum/earthquak/1/2j-1-2.html, 2017.

Coffey, J., “What are the Different Types of Earthquakes?” Universe Today, Space and astronomy news, Website: https://www.universetoday.com/82164/types-of-earthquakes/, 2019.

Construction and Planning Agency, Ministry of the Interior of Taiwan, Building Earthquake-Resistant Design Specifications, 2011.

Construction and Planning Agency, Ministry of the Interior of Taiwan, Building Foundation Design Specifications, 2001.

Drucker, D. C., “Some implications of work hardening and ideal plasticity,” *Quarterly of Applied Mathematics*, Vol. 7, No. 4, pp. 411-418, 1950.

Google Earth, Website: http://www.google.com/earth/index.html, 2021.

Hansen, J. B., “A Revised and Extended Formula for Bearing Capacity,” *Danish Geotechnical Institute Bulletin*, No. 28, Copenhagen pp. 5-11, 1970.

Hill, R., “Acceleration waves in solids,” *Journal of the Mechanics and Physics of Solids*, Vol. 10, pp. 1-6, 1962.

Hsu, Tse-Shan, *Capturing Localizations in Geotechnical Failures*, Ph.D. Dissertation, Civil Engineering in the school of Advanced Studies of Illinois Institute of Technology, 1987.

Hsu, Tse-Shan, Chang-Chi Tsao, and Chihsen T. Lin, "Localizations of Soil Liquefactions Induced by Tectonic Earthquakes," *The International Journal of Organizational Innovation*, Vol.9, No. 3, Section C, pp. 110-131, 2017.

Hsu, Tse-Shan, Cheng-Chieh Ho, "Shear Banding Induced Seismic Building Tilting Failure and Its Control," *International Journal of Organizational Innovation*, Vol. 9, No. 1, pp. 264-281, 2016.

Hsu Tse-Shan, Yi-Ju Chen, Zong-Lin Wu, Yi-Lang Hsieh, Jiann-Cherng Yang, Yi-Min Huang, "Influence of Strain Softening and Shear-band Tilting Effect on the Maximum Earth Pressure of Retaining Walls," *International Journal of Organizational Innovation*, Vol. 14, No. 1, pp. 45-86, 2021.

Hsu, Tse-Shan, Da-Jie Lin, Tsai-Fu Chuang and Yi-Min Huang, “Influence of Shear-Banding Effects on the Ultimate Bearing Capacity Equation of Foundation,” The International Journal of Organizational Innovation, Vol. 14. No. 13, pp. 205-233, January 2022.

Mandel, J., “Conditions de Stabilite et Postulat de Drucker,” In *Rheologie et Mechanique des Sols* (Edited by J. Kravtchenko and P. M. Sirieys), Springer, 1966.

McCarthy, David F., *Essential of Soil Mechanics and Foundations: Basic Geotechnics*, 7th Edition, Pearson Prentice Hall, pp. 346-349, 2007.

Meyerhof, G. G., "Ultimate bearing capacity of footings on sand layer overlying clay," *Canadian Geotechnical Journal*, Vol. *11*, pp. 223-229, 1951.

Meyerhof, G. G., Some Recent Research on the Bearing Capacity of Foundations," CGJ, Ottawa, Vol. 1, No. 1, pp. 16-26, 1963.

Prandtl, L. "Über die Härte, plastischer Körper, (On the Hardness of Plastic Bodies)," *Nachr. Kgl. Ges Wiss Gōttingen, Math-Phys. Kl.*, pp. 74, 1920.

Prevost, J. H., *Soil Stress-Strain-Strength Models Based on Plasticity Theory*, Ph.D. Dissertation, Department of Civil Engineering of Stanford University, 1974.

Rice, James R., "The Localization of Plastic Deformation," in *Theoretical and Applied Mechanics, Proceedings, 14th International Congress of Theoretical Applied Mechanics*, ed. Koiter, W. T., North-Holland, Inc., Amsterdam, pp. 207-220, 1977.

Rice, J. R., "The Localization of Plastic Deformation," in Theoretical and Applied Mechanics (Proceedings of the 14th International Congress on Theoretical and Applied Mechanics, Delft, 1976, ed. W.T. Koiter), North Holland, Amsterdam, Vol. 1, pp. 207-220, 1976.

Rudnicki, J. W., and Rice, J. R., "Conditions for the Localization of Deformation in Pressure-Sensitive Dilatant Materials," *Journal of the Mechanics and Physics of Solids*, Vol. 23. pp. 371-394. 1975.

Terzaghi, K., "Evaluation of Coefficient of Subgrade Reaction," Geotechnique, Vol. 5, No. 4, pp. 207-326, 1943.

Valanis, K. C., "Banding and stability in plastic materials," *Acta Mech.* Vol. 79, pp. 113-141, 1989.

Vesic, A. S., Analysis of Ultimate Loads of Shallow Foundation," *Journal of Soil Mechanics and Foundation Engineering, ASCE*, Vol. 99, SM1, pp. 45-73, 1973.